

Electron Diffraction 1927-1977

Invited and contributed papers from the
International Conference on Electron
Diffraction held in London,
19-21 September 1977

Edited by P J Dobson, J B Pendry and
C J Humphreys

Conference Series Number 41
The Institute of Physics
Bristol and London

Contents

v Preface

Chapter 1: Dynamical theory

- 1–12 The dynamical theory of electron diffraction
INVITED *A Howie*
- 13–17 Band theory in high-energy electron diffraction and the zone axis critical-voltage effect
B F Buxton and P T Tremewan
- 18–22 Diffraction patterns in an axial direction and structure of the dispersion surfaces in cross-grating orientation
Y Uchida, F Fujimoto, K-H Katerbau and M Wilkens
- 23–28 Linear combinations of Gauss-type orbitals and plane waves in the many-beam problem of high-energy electron diffraction
K Kambe
- 29–33 On the correspondence between atomic or molecular orbitals and Bloch functions in 2-d high-energy electron diffraction
B F Buxton, J E Loveluck and J W Steeds
- 34–40 Algebraic approaches to N -beam theory
A C Hurley, A W S Johnson, A F Moodie, P Rez and J R Sellar
- 41–46 A comparison of multislice and many-beam calculations
M D Shannon
- 47–49 Perturbation calculations in Bethe's dynamical theory of electron diffraction
A Hussein and H Wagenfeld
- 50–56 Electron diffraction contrast in the non-symmetric Laue case
D K Saldin, M J Whelan and C J Rossouw
- 57–60 Comparison of conventional and scanning transmission electron microscopy, with particular reference to atom images under dark field
R Uyeda and N Tanaka
- 61–67 Multiple inelastic scattering and dynamical diffraction
P Rez
- 68–73 A transmission study of 15 MeV electrons in silicon single crystals
E Worm, U Schiebel, A Neufert and G Clausnitzer
- 74–78 Experimental aspects of electron channelling patterns in scanning electron microscopy
T Yamamoto

- 79–83 The origin of the defect Kikuchi band from a thin crystal in electron diffraction
Y Nakai
- 84–87 Anomalous contrast of Kikuchi bands in RHEED from evaporated thin layers on Ge
Y Ishikawa, T Hanabusa, T Kawamura and T Ichinokawa

Chapter 2: Diffuse scattering

- 88–97 Short-range-order diffuse scattering from disordered alloys
INVITED *D Watanabe*
- 98–103 Disordering of Mg_3Cd under electron irradiation
E P Butler
- 104–108 The analysis of short-range order in some doped fluorite ceramics by electron diffraction
B Hudson and P T Moseley
- 109–115 Dynamical diffraction from periodic arrays of dislocations
P Rez

Chapter 3: Structure factor and symmetry determination

- 116–128 Accurate structure factor and symmetry determination
INVITED *P Goodman*
- 129–134 Convergent-beam diffraction in the Oxford high-voltage electron microscope
A F Moodie, C J Humphreys, D Imeson and J R Sellar
- 135–139 On the observation of dynamically forbidden lines in two- and three-dimensional electron diffraction
J W Steeds, G M Rackham and M D Shannon
- 140–144 Analysis of electron diffraction Kossel patterns
A Ichimiya and G Lehmpfuhl
- 145–149 The crystal potential in electron diffraction and in band theory
D J Smart and C J Humphreys
- 150–155 Theoretical and experimental studies of Bloch wave channelling
J Gjønnes and J Taftø
- 156–166 Crystal structure determination using electron diffraction
INVITED *J M Cowley*
- 167–171 Determination of crystal structure factors and temperature parameters by using dynamical effects in electron diffraction
H Hirono, K Mihama and A Ichimiya

- 172–177 The study of topochemical conversions and phase transitions in organic molecular crystals by electron diffraction
G M Parkinson, W Rees, M J Goringe, W Jones, S Ramdas, J M Thomas and J O Williams
- 178–181 Electron diffraction from a metastable phase of gold and germanium (gold 27 at.% germanium)
G M Rackham and J W Steeds
- 182–187 Electron diffraction patterns and high-resolution imaging from long-period polytypes in rare-earth trialuminides
M Gasgnier, G Schiffmacher and P Caro
- 188–194 Fine structure of the flux distribution of electron waves in crystal lattices near Bragg reflecting conditions
H Hashimoto and H Endoh
- 195–200 Accurate crystallographic information from precipitates in 316 and related stainless steels
K E Cooke, N Evans, L Stoter and J W Steeds
- 201–204 On the relationship between string integrals and the appearance of CB and BC zone axis patterns
K K Fung and J W Steeds

Chapter 4: Low-energy electron diffraction

- 205–217 Advances in LEED theory
INVITED *J B Pendry*
- 218–222 Temperature dependence of the LEED Kikuchi pattern and surface reconstruction of MgO (001) cleavage face
Y Murata and S Murakami
- 223–227 The variation of secondary electron emission under surface state resonance conditions in MEED
T Kawamura, T Ichinokawa, Y Watanabe and H Wada
- 228–232 Surface state resonance of the Kikuchi pattern in low-energy electron diffraction
S Murakami and Y Murata
- 233–238 Secondary electron emission spectroscopy in relation to low-energy electron diffraction
R F Willis
- 239–253 Electron diffraction in the medium-energy range
INVITED *D Aberdam*
- 254 Experimental and theoretical LEED spectra from W (001)
J Kirschner and R Feder

- 255–260 Inelastic LEED at the beam emergence condition: Al (100)
A E Hughes, K Senkiw and P J Dobson
- 261–269 Low-energy electron diffraction from disordered surfaces
W Moritz
- 270–280 A review of surface crystallography by low-energy electron diffraction
INVITED *S Y Tong*
- 281–286 Electron spin polarisation in LEED from Au (110)
N Müller, D Wolf and R Feder
- 287–294 Polarised LEED using a GaAs spin polarised electron source
W N Unertl, R J Celotta and D T Pierce

Chapter 5: Instrumentation

- 295–312 Instrumentation for electron diffraction
INVITED *T Mulvey*
- 313–318 RHEED and THEED patterns and dark-field microscopy in a UHV SEM
J A Venables, C J Harland and A P Janssen
- 319–323 The application of a digital scanning electron diffractometer to radiation-sensitive materials
W R K Clark, J N Chapman, A M MacLeod and R P Ferrier
- 324–328 The use of channel electron multipliers in gas electron diffraction experiments of short duration
A P Rood
- 329–334 Measurement of THEED intensity from adsorbed xenon monolayers
P S Schabes-Retchkiman and J A Venables

Chapter 6: Defect structure

- 335–349 Study of crystal defects by diffraction contrast in the electron microscope
INVITED *P B Hirsch*
- 350–356 The nature and geometry of irradiation-induced defects in copper, molybdenum and zirconium
D K Saldin, A Y Stathopoulos and M J Whelan
- 357–362 The study of grain-boundary dislocations
R C Pond
- 363–369 Effects of interdiffusion on the misfit dislocation configuration and the moiré patterns of thin bimetallic films
A M Beers, E J Mittemeijer and R Delhez

- 370–374 HREM *in situ* observations of dynamical behaviour of dislocations
T Imura, H Saka and K Noda
- 375–380 Direct observation of the displacement cascades in Cu₃Au produced by fast-neutron irradiation
M L Jenkins, C A English and J M Titchmarsh
- 381–386 Theoretical and experimental images of small dislocation loops in BCC materials
C A English, B L Eyre, S M Holmes and R C Perrin
- 387–390 Interpretation of crystallographic structure domains obtained at low temperature in vanadium sesquioxides
R Ayroles and C Roucau
- 391–395 Many-beam diffraction contrast for two-dimensional defects in crystals: application to merohedral twins
M Fayard, D Gratias, R Portier and M Guymont
- 396 An electron diffraction study of dislocation glide and climb in double heterostructure (DH) GaAs material
G R Woolhouse and B Monemar

Chapter 7: Miscellaneous

- 397–401 Reflection electron diffraction on silicon carbide crystals: new developments for the study of polytypism
J-P Gauthier and P Michel
- 402–410 Electron microscopy and electron diffraction of electron-sensitive materials
L W Hobbs, D G Howitt and T E Mitchell
- 411–415 Information from rutile catalyst particles by convergent-beam electron diffraction
M D Shannon and J A Eades
- 416–422 The microstructure and micromechanisms of deformation in polyethylene single crystals and spherulites
P Allan, M Bevis, A Low and D Vesely
- 423–429 Developments in liquid electron diffraction
E Kálmán
- 430–434 An electron diffraction study of liquid metals
A S Brah, P J Dobson, N H March, B A Unvala and L Viridhee
- 435–440 A double-crystal electron interferometer
G M Rackham, J E Loveluck and J W Steeds
- 441–442 Author Index

Low-energy electron diffraction from disordered surfaces

W Moritz

Institut für Kristallographie und Mineralogie, Universität München, Theresienstrasse 41, 8000 München 2, Federal Republic of Germany

Abstract. Model calculations are presented of LEED intensities diffracted by a one-dimensionally disordered overlayer adsorbed on a well ordered substrate. Multiple scattering amplitudes are calculated by an extension of Beeby's multiple scattering method. The surface layers are divided into overlapping configurations of atoms, the diffraction of each of which is described by individual scattering amplitudes. In this way the surrounding of each adsorbed atom is divided into two parts: the immediate vicinity, in which multiple scattering is treated self-consistently, and the outer region which is represented by an averaged \mathbf{T} matrix. The results of the model calculations indicate that the intensities are not correctly described if only averaged \mathbf{T} matrices are used, and that in a first approximation the half-widths of the diffuse streaks observed in the experiment can be analysed using the kinematic theory.

1. Introduction

The investigation of adsorption phenomena on surfaces and surface reactions by means of low-energy electron diffraction shows that disordered structures are predominant. LEED provides a readily accessible tool in the experimental observation of lateral interactions between adsorbed atoms and two-dimensional phase transitions, which have recently become of theoretical interest (Doyen and Ertl 1975, Binder and Landau 1976). However, there remain some uncertainties in the usual interpretation of diffuse LEED patterns which neglect multiple scattering effects. It has been assumed that multiple scattering effects are unimportant as long as only the half-widths of the diffuse peaks are studied as a function of temperature and coverage with fixed energy and angles of incidence of the primary beam (Estrup and Anderson 1967, McKee *et al* 1973, Gerlach and Rhodin 1969, Carroll 1972, Ertl and Plancher 1975, Park and Houston 1969, Houston and Park 1970, 1971, Cowley and Shuman 1973, Ertl and Küppers 1970). The results of a few model calculations presented in this paper show that this assumption is rather well justified, and to a first approximation the half-widths of the strong peaks remain unchanged compared to the kinematic calculation and can be used to determine the statistical parameters by direct evaluation of the measured reflex profile. The shape of the angular profile may be strongly deformed by multiple scattering effects and, of course, a multiple scattering theory is necessary to get a correct description of the intensities (e.g. of the intensity changes during a phase transition) or if the calculated intensities of diffuse streaks have to be compared with the experiment in order to decide between two or more possible structure models.

The calculation of multiple scattering amplitudes from disordered surfaces can be done by an extension of Beeby's \mathbf{T} matrix formalism (Beeby 1968). The surface layers

are divided into overlapping configurations of atoms; the diffraction of each configuration is described by individual scattering amplitudes. In this way multiple scattering within the ordered substrate and the area of the adsorbed layer (as described above) is treated self-consistently, while an averaged scattering amplitude is taken for the remaining contributions. The use of configurations of atoms also has the advantage that statistical models, including nearest-neighbour and next-nearest-neighbour interactions, and even interactions between atoms further apart, can be used in the multiple scattering formalism.

Once the scattering amplitudes are calculated, the determination of the intensities and the angular reflection profiles follows the same lines as already described in the theory of diffuse x-ray diffraction (Jagodzinski *et al* 1978).

2. Model of the surface

The lattice-gas model is a reasonable model to describe a disordered adsorbed overlayer, and the specific model used here shows disorder in one direction only for the sake of simplicity (figure 1). The restriction to one-dimensional disorder is advantageous in that the correlation functions can be calculated analytically and an analytical

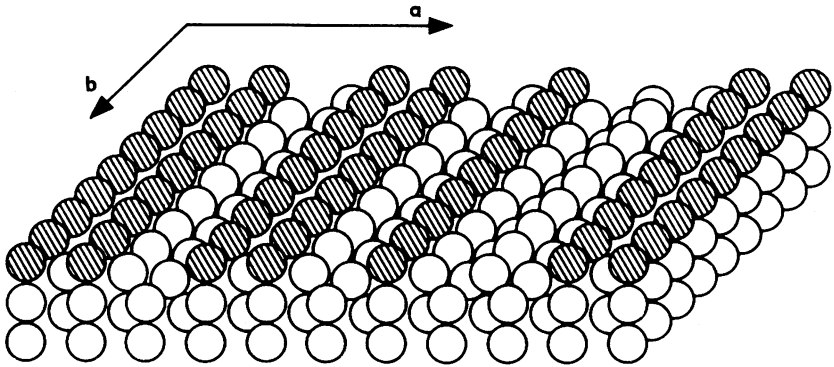


Figure 1. Model of the one-dimensionally disordered surface.

expression exists for the backscattered intensity. It is not believed that two-dimensional disorder produces completely new effects in the angular profiles. In addition, one-dimensionally disordered overlayers are quite frequently realised, such as oxygen on W(112) (McKee *et al* 1973, Ertl and Plancher 1975) and Ag(110) (Bradshaw *et al* 1972), Na on Ni(110) (Gerlach and Rhodin 1969), and the clean Au(110) surface (Wolf *et al* 1978).

If only nearest-neighbour interactions are assumed, the statistical distribution of the adsorbed chains of atoms is completely described by two parameters α_1 and α_2 , $p_{AA}(1) = (1 - \alpha_1)$, $p_{AB}(1) = \alpha_1$, $p_{BA}(1) = \alpha_2$, $p_{BB}(1) = (1 - \alpha_2)$, where A denotes an adsorbed chain and B a vacancy. $p_{AA}(1)$ denotes the probability that one chain of adsorbed atoms is followed by another one. The *a priori* probabilities p_n are given by the eigenvalue equation

$$\sum_m p_m p_{mn}(1) = p_n$$

and the correlation functions for all distances ja are simply given by $p_{mn}(j) = [\mathbf{P}(1)]_{mn}^j$ (where $j = 1, 2, \dots$) using the matrix

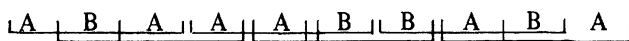
$$\mathbf{P}(1) = \begin{pmatrix} p_{AA} & p_{AB} \\ p_{BA} & p_{BB} \end{pmatrix}. \quad (1)$$

The correlation functions $p_{mn}(j)$ may also be expressed in terms of the eigenvalues λ_r of the matrix $\mathbf{P}(1)$ (Jagodzinski 1949, 1954)

$$p_{mn}(j) = \sum_r C_{mn}^{(r)} \lambda_r^j \quad (2)$$

in order to render summable the expression for the interference of amplitudes. The kind and position of diffuse peaks in the diffraction pattern is determined by the eigenvalues λ , which are generally complex and of modulus $|\lambda| \leq 1$. A detailed discussion on that topic is given by Jagodzinski *et al* (1978). In order to include next-nearest-neighbour interactions, four parameters are needed for describing the distribution of adsorbed chains: $p_{AAA} = \alpha_1$, $p_{ABA} = \alpha_2$, $p_{BAA} = \alpha_3$, $p_{BBA} = \alpha_4$. This results in an enlarged matrix $\mathbf{P}(1)$ and four eigenvalues λ , by which a 4×1 superstructure can be described.

The probabilities mentioned above are related to the occupancy of lattice sites by adsorbed atoms and can be used as input parameters in a kinematic theory of diffraction. The multiple scattering theory described below needs probabilities as input parameters, which are related to configurations of atoms, as the effective scattering amplitude is influenced by its neighbourhood. The effective scattering amplitude represents all scattering processes which end in that atom. In a first approximation only the nearest neighbours are included in these configurations and the disordered surface is constructed by overlapping configurations



each one getting a different scattering amplitude which is related to the central atom of the configuration. The matrix of probabilities described above has therefore to be re-defined as the set of configurations:

	AAA	AAB	BAA	BAB	ABA	ABB	BBA	BBB
AAA	$(1-\alpha_1)$	α_1	0	0	0	0	0	0
AAB	0	0	0	0	α_2	$(1-\alpha_2)$	0	0
BAA	$(1-\alpha_1)$	α_1	0	0	0	0	0	0
BAB	0	0	0	0	α_2	$(1-\alpha_2)$	0	0
ABA	0	0	$(1-\alpha_3)$	α_3	0	0	0	0
ABB	0	0	0	0	0	0	α_4	$(1-\alpha_4)$
BBA	0	0	$(1-\alpha_3)$	α_3	0	0	0	0
BBB	0	0	0	0	0	0	α_4	$(1-\alpha_4)$.

(3)

This matrix becomes degenerate, still having the same eigenvalues λ_1 to λ_4 , while λ_5 to λ_8 vanish. Of course, this is independent of the size of the configuration and the dimensions of the matrix, as long as the same surface is described.

The connection between the probabilities or correlation functions and thermodynamic quantities like interaction energies etc will not be discussed here, as we only need those probabilities which can be determined by comparison with the experimental diffraction picture.

3. Multiple scattering theory

Since the details of the theory are given elsewhere (Moritz *et al* 1978), only a brief description will be outlined here. As mentioned above, the effect of multiple scattering is that each atom with a different neighbourhood gets a different scattering amplitude, which becomes explicitly dependent on the incoming and outgoing wave vectors \mathbf{k} and \mathbf{k}' . Within a single layer the contribution from the neighbouring atoms to the total scattering amplitude is so strong in most cases that a series expansion fails, while between the layers the strong damping above the plasmon threshold permits perturbative methods (Pendry 1971). For intra-layer scattering the sum over lattice points is best done in direct space and, usually, all lattice points within a circle of about 10–15 interatomic distances have to be included to reach convergence. However, the main contribution arises from single scattering and multiple scattering between nearest or next-nearest neighbours (Moritz *et al* 1978). These principles remain valid in the case of both ordered and disordered surfaces.

On a disordered surface there are no equivalent sites and the scattering from a layer or a subplane cannot be represented by a single \mathbf{T} matrix. In order to facilitate the solution of the problem the averaged \mathbf{T} matrix approximation (Ehrenreich and Schwartz 1976) – well known in the theory of the electronic structure of binary alloys – could be used. It is also employed by Duke and Liebsch (1974) in their application to disordered overlayers. In their work the main difficulty arises in trying to incorporate correctly short-range order in the multiple scattering series. In the method used here the surrounding of an atom is divided into an 'area of multiple scattering', which includes nearest or next-nearest neighbours, and the outside region, which is represented by an averaged \mathbf{T} matrix. For each of the possible configurations inside the 'area of multiple scattering' a different scattering amplitude is calculated. In this way two main difficulties are overcome. First, the most important part of the multiple scattering amplitude (caused by the immediate vicinity of an atom) is treated self-consistently, and second, there is no restriction to a random distribution of the adsorbed atoms (high-temperature limit) as any statistical model is easily incorporated in the multiple scattering formalism.

The formalism best suited for introducing disorder is the \mathbf{T} matrix method as given by Beeby (1968), where the sum over lattice points and layers is done in real space, which has the advantage that the \mathbf{T} matrices themselves depend only on the incoming wave vector \mathbf{k} , and the set of equations has to be solved only once to get the intensities in all outgoing directions \mathbf{k}' .

The final formula is given by

$$T^{m,\nu}(\mathbf{k}) = t_{m,\nu}(k) + t_{m,\nu}(k) \sum_{\mu} \sum_n G_{mn}^{\mu\nu}(\mathbf{k}) T^{n,\mu}(\mathbf{k})$$

$$G_{mn}^{\mu\nu}(\mathbf{k}) = \sum_{\mathbf{R}}^{|R| \leq r} G(\mathbf{R} + \mathbf{d}_{\mu} - \mathbf{d}_{\nu}) \exp[-i \mathbf{k}(\mathbf{R} + \mathbf{d}_{\mu} - \mathbf{d}_{\nu})] p_{mn}(\mathbf{R})$$

$$+ \sum_{\mathbf{R}}^{|R| > r} G(\mathbf{R} + \mathbf{d}_{\mu} - \mathbf{d}_{\nu}) \exp[-i \mathbf{k}(\mathbf{R} + \mathbf{d}_{\mu} - \mathbf{d}_{\nu})] p_n \quad (4)$$

where the indices ν, μ denote the different layers, and the indices n, m stand for the different configurations. $p_{mn}(\mathbf{R})$ are the sequence probabilities as given in equation (3) and, for convenience, the angular momentum indices L, L' of the electron propagator matrices and the scattering matrices have been suppressed. For the special model of a half-covered surface, one sort of adsorbate atoms and N possible configurations, the atomic scattering matrices are

$$t_{m,\nu}(k) = \begin{cases} t_A = (1/k) \exp(i \delta_{l,A}) \sin \delta_{l,A} \delta_{L,L'} & (\nu = 1, m = 1, \dots, N/2) \\ 0 & (\nu = 1, m = (N/2) + 1, \dots, N) \\ t_S = (1/k) \exp(i \delta_{l,S}) \sin \delta_{l,S} \delta_{L,L'} & (\nu \geq 2). \end{cases} \quad (5)$$

$\delta_{l,A}$ and $\delta_{l,S}$ are the phase shifts of the adsorbate and substrate respectively. The system of equations (4) is not solved directly because of the dimension of the matrix to be inverted. Therefore a perturbative solution has been used in which first an averaged \mathbf{T} matrix is calculated and then the deviations from the average are obtained by an iteration scheme described in the appendix of the work by Moritz *et al* (1978). The diffracted intensity can be written (Jagodzinski *et al* 1978) as

$$I(\mathbf{k}, \mathbf{k}') = RM \sum_j \overline{FF_j^*} \exp[-i(\mathbf{k} - \mathbf{k}') \cdot \mathbf{a}_j] \quad (6)$$

where R_L is a normalisation factor, M the number of unit cells, and $\overline{FF_j^*}$ the averaged structure factors

$$\overline{FF_j^*} = \sum_{m,n} p_m p_{mn}(j) F_m(\mathbf{k}, \mathbf{k}') F_n^*(\mathbf{k}, \mathbf{k}'). \quad (7)$$

$F_m(\mathbf{k}, \mathbf{k}')$ represents a generalised structure amplitude and contains the sum over layers:

$$F_m(\mathbf{k}, \mathbf{k}') = \frac{-8\pi^2 i}{A k_{\perp}^1} \sum_{\nu} \sum_{L,L'} Y_L(\Omega_{\mathbf{k}'}) T_{LL'}^{m,\nu}(\mathbf{k}) Y_{L'}^*(\Omega_{\mathbf{k}}) \exp[i(\mathbf{k} - \mathbf{k}') \cdot \mathbf{d}_{\nu}]. \quad (8)$$

Using equation (2)

$$\overline{FF_j^*} = \sum_{m,n} \sum_r C_{mn}^{(r)} \lambda_r^j F_m F_n^* = \sum_r (B_r + i D_r) \lambda_r^j \quad (9)$$

the final formula for the diffracted intensity from the surface disordered in the x direction only is given (Jagodzinski 1949, 1954) by

$$I(\mathbf{k}, \mathbf{k}') = R_R M \left\{ \sum_r^{1,N} B_r \frac{1 - |\lambda_r|^2}{1 - 2|\lambda_r| \cos(A_1 + \phi_r) + |\lambda_r|^2} - 2D_r \frac{|\lambda_r| \sin(A_1 + \phi_r)}{1 - 2|\lambda_r|^2 \cos(A_1 + \phi_r) + |\lambda_r|^2} \right\} \sum_{g_y} \delta(k_y - k'_y + g_y)$$

where

$$A_1 = (\mathbf{k} - \mathbf{k}') \cdot \mathbf{a}$$

$$\lambda_r = |\lambda_r| \exp(i \phi_r)$$

4. Results and discussion

Two different models of disorder have been studied. In the first model $\alpha_1 = \alpha_2 = \alpha_3 = \alpha_4 = 0.8$ is assumed, which represents a half-covered surface with repulsive interactions between the adsorbed atoms (NN interactions only) and results in a (2×1) superstructure with broadened half-order and sharp integer-order reflections. In the second model, interactions between next-nearest neighbours have been added by setting $\alpha_1 = \alpha_4 = 0.8$ and $\alpha_2 = \alpha_3 = 0.4$. The surface is still half-covered and mainly

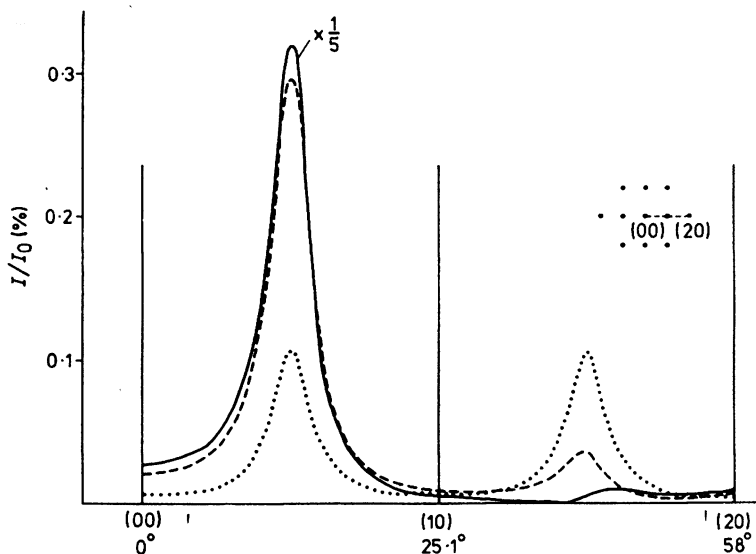


Figure 2. Kinematically calculated intensities showing the influence of the atomic differential cross section on angular reflection profiles. $\alpha_1 = \alpha_2 = \alpha_3 = \alpha_4 = 0.8$, $E_D = 50$ eV, $V_1 = 4$ eV, normal incidence: \cdots 1 phase shift (s-wave scattering); $---$ three phase shifts; $—$ four phase shifts. The position of the sharp integer-order reflections is indicated by the vertical lines.

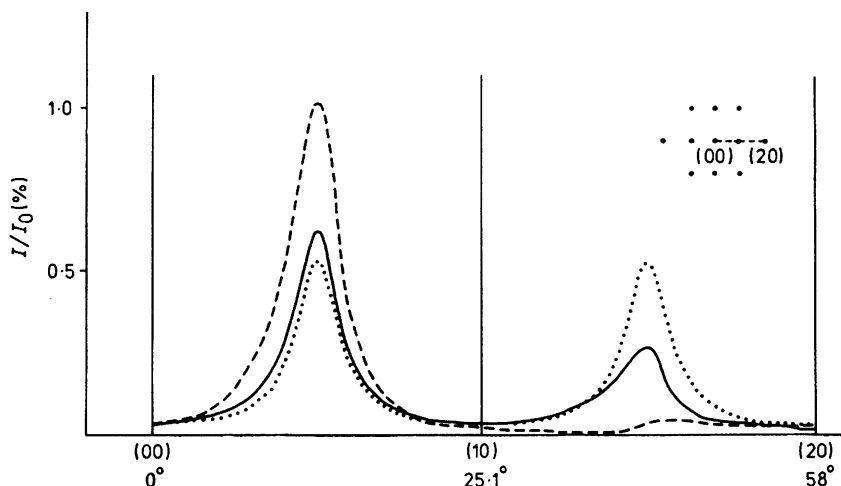


Figure 3. Dynamically calculated angular profiles for same model as in figure 2, taking into account four phase shifts and five layers: — nearest neighbours are included in the configurations for the uppermost three layers; - - - averaged \mathbf{T} matrices are used for all layers; ··· as in figure 2, without intensity scale.

pairs of chains are formed, resulting approximately in a (4×1) superstructure. The (110) face of silver has been chosen as substrate and the same phase shifts have been used for adsorbate and substrate, as different phase shifts do not seem to be relevant in these model calculations. Up to four phase shifts have been taken into account, which should be sufficient at 50 eV primary-beam energy. The crystal consists of five layers, of which the uppermost three are divided into configurations as described above; the damping parameter has been set at $V_i = 4$ eV.

Figure 2 shows the calculated reflection profiles with different numbers of phase shifts used. The suppression of the $(3/2, 0)$ reflection corresponds to a deep minimum in the atomic scattering amplitude of silver at $\theta = 140^\circ$ and $E_p = 50$ eV. The dotted lines in diagrams 2–4 are obtained by single scattering and s-wave scattering only (i.e. it is simply the Fourier transform of the correlation functions and represents the 'state of order' of the surface, lacking any individual scattering properties). Figure 3 shows that through the influence of multiple scattering the $(3/2, 0)$ reflection appears again, but this is not the case if averaged \mathbf{T} matrices only are used (broken curve). In that approximation the size of the configurations has shrunk to a single atom and the scattering properties of an adsorbed atom are described by a single \mathbf{T} matrix. This approximation is not sufficient to describe the intensities correctly.

For comparing the width of line profiles at half-intensities, even a kinematic calculation is sufficient. All prominent peaks show mainly the same shape; the very weak peaks are not used anyway in an experimental investigation. The same features are obtained with the second statistical model shown in figure 4. With different energies, rather different peak profiles are obtained. Nevertheless, the conclusion may be drawn that in an experiment the proper half-widths (that of the dotted line) could be measured approximately. However, the correct description of the intensities is only possible

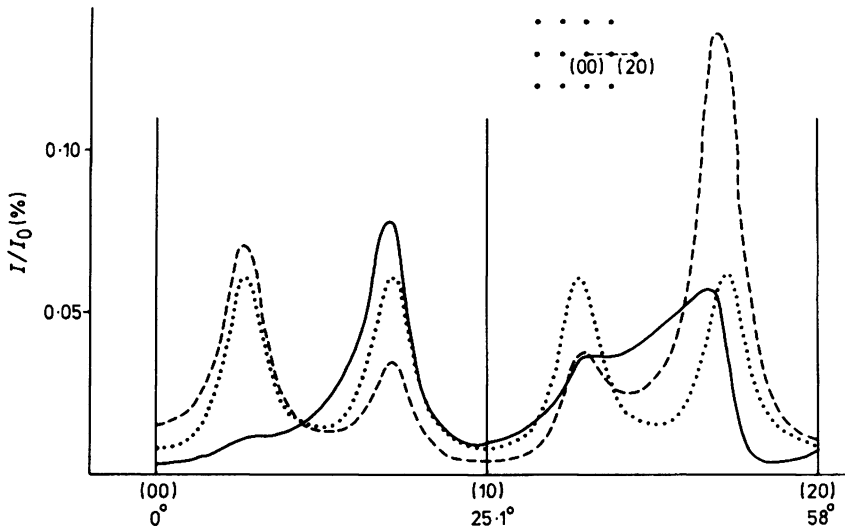


Figure 4. Dynamically calculated angular profiles at two different energies of the incident beam. Nearest neighbours are included in the configuration for the first three layers, and three phase shifts are used. — $E_p = 50$ eV; --- $E_p = 70$ eV. The statistical model includes next-nearest-neighbour interactions $\alpha_1 = \alpha_2 = 0.8$, $\alpha_3 = \alpha_4 = 0.4$ kinematic calculation with s-wave scattering.

with a rather lengthy multiple scattering formalism in which the neighbourhood of an atom is considered explicitly in different configurations and is not replaced by an average. The averaged **T** matrix is the starting value in the iteration scheme (Moritz *et al* 1978) used here to solve equation (4). This iteration scheme turned out to be poorly convergent; 5–8 iterations were necessary to reach convergence within an

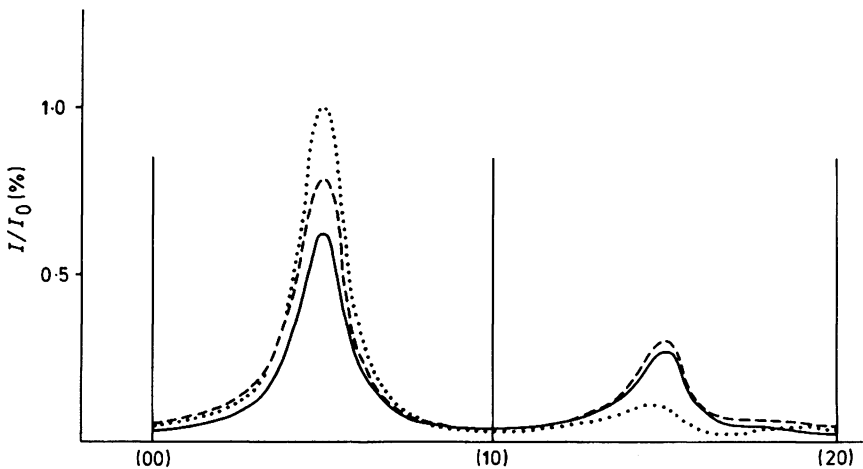


Figure 5. Convergence of the iteration procedure by which equation (4) is solved (same conditions as in figure 3): ... four iterations; --- five iterations; — seven iterations.

accuracy of 10%, which means that a direct solution would have been more efficient. The convergence of the iteration procedure is shown in figure 5.

In the few model calculations presented here only the nearest neighbours are included and this is probably not sufficient. Inclusion of the next-nearest neighbours is possible by making use of the symmetry properties of the propagator matrices at normal incidence and the degeneracy of the matrix of probabilities.

References

- Beeby J L 1968 *J. Phys. C: Solid St. Phys.* **1** 82–7
Binder K and Landau D P 1976 *Surf. Sci.* **61** 577–602
Bradshaw A M, Engelhardt A and Menzel D 1972 *Ber. Bunsen Ges.* **76** 500–7
Carroll C E 1972 *Surf. Sci.* **32** 119–38
Cowley J M and Shuman H 1973 *Surf. Sci.* **38** 53–9
Doyen G and Ertl G 1975 *J. Chem. Phys.* **62** 2957–66
Duke C B and Liebsch A 1974 *Phys. Rev.* **B9** 1126–49 1150–9
Ehrenreich H and Schwartz L M 1976 *Solid St. Phys.* **31** 150–286
Ertl G and Küppers J 1970 *Surf. Sci.* **21** 61–75
Ertl G and Plancher M 1975 *Surf. Sci.* **48** 364–72
Estrup P J and Anderson J 1967 *Surf. Sci.* **8** 101–14
Gerlach R L and Rhodin T N 1969 *Surf. Sci.* **17** 32–68
Houston J E and Park R L 1970 *Surf. Sci.* **21** 209–23
— 1971 *Surf. Sci.* **26** 269–85
Jagodzinski H 1949 *Acta Crystallogr.* **1** 201–7, 208–14, 298–304
— 1954 *Acta Crystallogr.* **7** 17–25
Jagodzinski H, Moritz W and Wolf D 1978 *Surf. Sci.* to be published
McKee C S, Perry D L and Roberts M W 1973 *Surf. Sci.* **39** 176–205
Moritz W, Jagodzinski H and Wolf D 1978 *Surf. Sci.* to be published
Park R L and Houston J E 1969 *Surf. Sci.* **18** 213–27
Pendry J B 1971 *J. Phys. C: Solid St. Phys.* **4** 2501–13, 2514–23, 3095
Wolf D, Jagodzinski H and Moritz W 1978 *Surf. Sci.* to be published